

Performance Review of the VSC-HVDC Based Controllers

J. K. Muriuki, C. M. Muriithi, L. M. Ngoo, G.N. Nyakoe

Abstract— The Voltage Source Converters, High Voltage Direct Current (VSC-HVDC) system is the most preferred alternative technology for transmission and distribution of electrical power due to its intrinsic distinctiveness in independent control of active and reactive power. In addition, it has the capability to connect weak system to the networks such as the wind farm and other renewable energy sources. The cascaded control scheme in VSC-HVDC is a two level control system that consists of outer controllers and the inner current controllers. The outer controllers include the active and reactive power controller, frequency controller, AC-voltage controller and the DC-voltage controller. The inner current controller is the inner part of the cascaded control strategy and function in conjunction with the outer controllers. It needs to be very fast as compared to the outer controllers so as to achieve control system stability. This analysis involves the proposed controllers using mathematical model to investigate the performance characteristics in the control of active and reactive power, and DC voltage. Also analyzed is the behavior of the converters under transient fault at the VSC buses. The model is implemented in DigSilent Power Factory and the results indicate some good improvement in the controllability of DC voltage, active and reactive power.

Keywords—Inner Current Controllers, Outer Controllers, Power System Stability, Voltage Source Converter, High Voltage Direct Current.

I. INTRODUCTION

Voltage Source Converter, High Voltage Direct Current (VSC-HVDC) System is the most preferred transmission and distribution technology of choice due to its inherent characteristics in the independent control of active and reactive powers. The voltage source converter (VSC) behaves like a synchronous machine and can generate AC voltage at the required frequency therefore, finding applications like in

connection of wind farms. VSC-HVDC system utilizes four outer controllers and one inner controller to ensure that power, frequency and voltage are maintained within the desired levels. It is critical that the design of controllers and their selection in VSC system is done for better performance. Due

to these features, the analysis of VSC-HVDC control system is carried out in this study to assess its performance on the independent control of active and reactive power under normal and fault condition.

Basically, VSC-HVDC system involves the study of the control system with its controllers. The inner current controller which is also referred to as vector current control is tuned with the goal of achieving fast response of the system and optimizes the plant output. The tuning of the VSC controllers is based on the principle adopted for the basic electrical derives [1].

The two common power flow control types are direct power control and vector current control. The former control method is where the active power is controlled by controlling the phase-angle shift between the converter voltage and the AC system voltages while the reactive power is controlled by varying the converter output voltage magnitude with respect to system demand. Because of disadvantages like variable switching frequency and necessity of fast conversion and computation, the use of direct power control is not very common [2]. Vector current control is the most preferred control strategy because of its excellent dynamic performance and intrinsic protection against overcurrent. It also has the ability that makes it possible to independently control active and reactive powers through decoupled control ability. The decoupling of quantities allows the implementation of a cascaded control strategy which has improved dynamic performance.

As previously mentioned, Cascaded control strategy in VSC-HVDC is a two level control system that consists of outer controllers and the inner current controllers. The controllers used are PI controllers. Basically, PI controllers are PQ controllers whose responsibilities are to regulate the active and reactive power between the converters and the grid. PI controllers are designed based on the transfer function of VSC model [3]. The main aim of PQ- control is to regulate the active and reactive power exchange between the converter and the grid. [4] Derived the VSC models based on system parameters and basic circuit equations, which means the system variables need to be known in advance. [5] Obtained the multiterminal VSC-HVDC model via small signal analysis. VSC-HVDC system can be used to connect a wind farm because of its independent control of active and reactive powers. However, according to [6], VSC-HVDC system of transmission is cost effective for distances between 60km to 100km and is implemented in this study because the

J. K. Muriuki, Department of Electrical Engineering, JKUAT, jkmuriuki4@gmail.com;

C. M. Muriithi, Dept. of Electrical & Power Engineering, Technical University of Kenya, Kenya. 0721 791 736, cmainamuriithi@gmail.com;

L. M. Ngoo, Dept. of Electrical & Electronic Engineering, Multimedia University, Kenya. 0722 490 180, livingngoo@gmail.com;

G. N. Nyakoe, Dept. of Electrical & Electronic Engineering, Jomo Kenyatta University of Agriculture and Technology, Kenya. nyakoe@eng.jkuat.ac.ke

transmission distance is beyond 60Km. However, for distances less than 60km, Alternating current (AC) transmission is cheaper and has better returns on investment than direct current (DC) transmission.

This paper analyzes the proposed VSC-HVDC controllers to demonstrate how effectively the system can independently control the active and reactive power and DC voltages between the grid and the converter both under normal and during fault condition. The simulations obtained indicate increase in active and reactive power control thus increasing the system reliability and stability. The proposed controller's combination relies on the accurately designed outer and inner controllers thus reducing the oscillations quickly and ensuring that system stability is reached within a very short time. The detailed model of the VSC-HVDC converter and the controllers are implemented in DigSilent PowerFactory software.

II. MATHEMATICAL MODELLING OF THE VSC-HVDC SYSTEM

Before discussing about modelling of the VSC-HVDC system, it is important to briefly highlight its constituents. Basically, a VSC-HVDC transmission system consists of converter valves, phase reactors, filters, power transformers, DC capacitors and DC lines. Though all components are important, converters play the biggest role of converting AC to DC (rectifier) and DC to AC (inverter). The two converters can be connected either via a dc cable, or an over head line or in back-to back connection depending on the application.

Normally, the converter valves are built with insulated gate bipolar transistor (IGBT) power semiconductors and are provided with R-C snubbers and series R-L elements to reduce dv/dt and di/dt stresses that occur during the quick switching transitions. IGBTs operate at very high frequencies and find many applications such as in high-power high frequency circuits as opposed to Field Effect Transistor (FET) that operate only in low-power high frequency circuits. Phase reactors have large inductance and small resistances to enable regulation of active and reactive power to the AC grid and also protect the transformer against high frequency harmonics [7]. Transformers are used to convert voltages to values suitable for the converters while shunt filters are used to filter out the generated harmonics and prevent them from entering the AC system. The DC capacitor is for maintaining the DC voltage at constant value and it should be carefully selected to avoid large ripples in the DC voltage.

In this study, vector control strategy has been utilized due to its inherent ability to independently control active power and reactive power and also has the ability to maintain DC voltage constant. The vector control strategy for VSC-HVDC starts from the mathematical modeling of VSC-HVDC system in dq-reference frame. The VSC can be represented by a controlled voltage source for the AC side as in figure 2.0 (a) and a current source for the DC side as in figure 2.0 (b).

According to Kirchhoff's Voltage Law (KVL), the algebraic sum of the voltages across any set of branches in a closed loop

is zero. Therefore applying Kirchhoff's voltage law across the reactor (L) and the resistor (R) the following equation holds true.

$$L \frac{di_{abc}}{dt} = V_{abc} - U_{abc} - Ri_{abc} \quad (1)$$

Where V_{abc} and U_{abc} are the Grid AC voltage and converter AC side output voltage in abc reference frame, i_{abc} AC current through the reactor in abc reference frame, R - Reactor resistance, L-Reactance inductance.

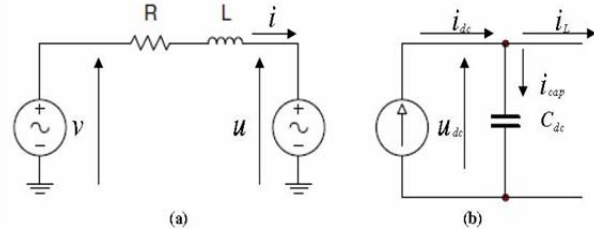


Fig. 1 Equivalent circuit of VSC station.

Using the coordinate transformation technique known as Clark transformation below;

$$\frac{2}{3} \begin{bmatrix} 1 & -\frac{1}{2} & -\frac{1}{2} \\ 0 & \frac{\sqrt{3}}{2} & -\frac{\sqrt{3}}{2} \end{bmatrix} \quad (2)$$

The time varying three phase quantities in equation 1 above are transformed to vectors in a two coordinate (α, β) system as shown below.

$$\begin{cases} x_\alpha \\ x_\beta \end{cases} = \frac{2}{3} \begin{cases} 1 & \cos \frac{2\pi}{3} & \cos \frac{4\pi}{3} \\ 0 & \sin \frac{2\pi}{3} & \sin \frac{4\pi}{3} \end{cases} \quad (3)$$

This clark transformation gives the advantage of dimension order reduction. Hence,

$$L \frac{di_{\alpha\beta}}{dt} = V_{\alpha\beta} - U_{\alpha\beta} - Ri_{\alpha\beta} \quad (4)$$

By using transformation angle from the system phase measurement at the PLL the electrical quantities are further transformed from the (α, β) stationary coordinate system quantities to a rotational dq-reference frame equivalent quantities by applying the following park transformation matrix.

$$\begin{cases} \cos\theta & \sin\theta \\ -\sin\theta & \cos\theta \end{cases} \quad (5)$$

By using the above park transformation matrix, the rotational dq-reference quantities gives the equation 6 below.

$$\begin{cases} x_d \\ x_q \end{cases} = \begin{cases} \cos\theta & \sin\theta \\ -\sin\theta & \cos\theta \end{cases} \begin{cases} x_\alpha \\ x_\beta \end{cases} \quad (6)$$

Hence, equation 4 is transformed to;

$$L \frac{di_{dq}}{dt} = V_{dq} - U_{dq} - \{R + j\omega L\}i_{dq} \quad (7)$$

Equation 7 can be split into two individual equations with d and q-axes. They show the relationship between the converter voltages and input currents in dq-reference frame thus completing the modeling for VSC-HVDC converter station.

III. PROPOSED VSC-INNER CURRENT CONTROLLER

The inner current controller is interlinked with the outer controllers and is proposed to ensure that it has a very fast response compared to the outer controllers for system stability. According to [8] the inner current control is implemented in a dq-coordinate system. The phase locked loop (PLL), which

provides the reference angle of the dq transform, normally enables the d-axis to be aligned with the voltage vector at the point of common coupling (PCC) so as to achieve an independent control of real and reactive power [9]. The inner current control loop has two PI regulators each for the d and q axis reference currents. The input current to the rectifier and the output current from the inverter is measured and compared with the reference current values and the error (Err) signal is fed to the controllers to produce switching signals to the PWM converters. The current control loop is as shown in fig.2.

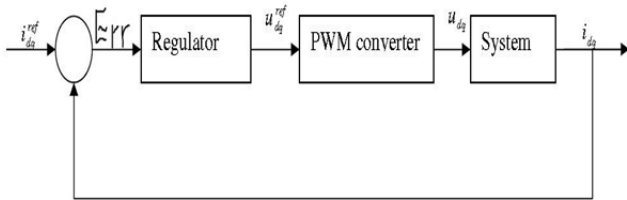


Fig. 2 Inner current control loop

The regulator is the proportional and integral controllers (PI). As a result of the dq transformations produced by the DC vectors, the PI is able to reduce the steady state error signal to zero. The PI regulator is represented by the equation below

$$Kp \left\{ 1 + \frac{1}{sTi} \right\} \quad (8)$$

The PWM produces the output voltage. In PWM the switching frequency is expected to be much larger than the system frequency. In this study, converter switching frequency of 5000Hz is chosen. The high frequency chosen reduces the size of the filters required to eliminate the harmonics generated.

The inner current controller proposed is tuned to achieve fast response of the system [1]. In this case, the inner loop is tuned according to the optimum modulus criterion. From fig.2, a transfer function with the equation below is obtained through the modulus optimum criteria.

$$Go(s) = Kp \left\{ \frac{1+sTi}{sTi} \right\} \left\{ \frac{1}{1+sTi} \right\} \left\{ \frac{1}{R+sL} \right\} \quad (9)$$

IV. PROPOSED VSC OUTER CONTROLLERS

Normally, a VSC-HVDC system has four outer controllers. In this study case, only three outer controllers are discussed. These are the Active power controller, Reactive power controller and the DC voltage controllers. A two terminal VSC-HVDC system has a rectifier and an inverter. The rectifier station operates as a power control mode to control active power drawn from the AC grid and at the same time controls the reactive power compensated to the grid. It also has the capability to control AC grid voltage directly. The inverter station has the responsibility of ensuring that the DC link voltage is maintained at the desired specific level otherwise the active power flow balance between the two converters may result into power imbalance.

The outer controllers need to be properly tuned so that to damp the system oscillations and attain system stability. The outer controllers generate the reference d-component currents and q-component currents. The current values are later fed into the faster inner current controller which gives d-q component voltage values that are injected into PWM generator and into the system. In [10], all the outer controllers are implemented by a PI controller where the difference between the reference values and the actual value is fed into the controller as the d-q reference currents.

A. ACTIVE AND REACTIVE POWER CONTROLLERS

The aim of PQ controllers which are essentially PI controllers is to regulate the active and reactive power exchange between the converters. The reactive power balance in a grid largely relies on the voltage levels on the grid and any deviation will lead to system instability. The P and Q powers are calculated from the grid and compared with the reference values and the error signal is made to pass through PI regulator. The PI controllers create the reference d and q currents which are fed to the inner current controllers. [11], the structure and transfer functions of active and reactive power control are as shown in fig. 3 below.

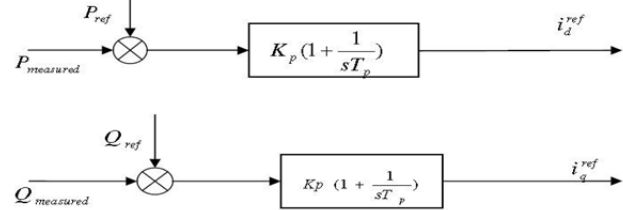


Fig. 3.Active and reactive power controllers loop

In a VSC HVDC system, every converter can be selected to independently control its reactive power injection into the power system. Similarly, only one converter is selected at a time to independently control the active power and the DC voltage respectively. In [12], the converter selected to control the DC voltage is called the slack converter because it usually compensates the losses in the DC network and therefore has a similar function as a slack node in an AC grid. The outer control loop of the VSC converter controls the active and reactive power. The PI controller used for the active power controller has the same structure as the PI controller. [13], states that there is no general rule for tuning the controllers and therefore in this study, trial and error method was carried out to yield best responses. The selected parameters for the controllers are the KP=10 and the TI=0.1 respectively. Further, it is important to note that the active and reactive control depend on the independent control of id and iq current components. The equation below shows that the active power is independent of the coordinate system and is represented by dq-reference.

$$Pt = \frac{3}{2} \{ Vdi_d + Uqi_q \} + Volo \quad (10)$$

In a balanced system, the zero component is assumed to be zero, thus the equation becomes;

$$Pt = \frac{3}{2}\{Vdi_d + Uqi_q\} \quad (11)$$

Since the active and reactive powers depends on the independent control of i_d and i_q currents, then, equation 11 is split into two equations as follows:

$$P = \frac{3}{2}Vdi_d \quad (12)$$

$$Q = \frac{3}{2}Vqi_q \quad (13)$$

The above two equations shows that the active and reactive power controls depend on the independent control of i_d and i_q currents components.

B. DC VOLTAGE CONTROLLER

DC voltage controller is responsible for controlling the active and reactive powers between the converters. In VSC- HVDC system, the DC voltage control is implemented through the integration of the inner current loop and the outer control loops. The two must work concurrently for power flow balance between the converters and subsequently between the grids. As previously mentioned, the inner current controller should be fast enough in order to get the best system response as based on [11]. In order to derive the DC voltage control loop, some assumptions were made. Assuming a lossless converter, the power into the converter is equal to the power output from the converter.

Therefore, based on this assumption, the two equations hold true.

$$P = \frac{3}{2}Vdi_d \quad (14)$$

$$Q = -\frac{3}{2}Vdi_q \quad (15)$$

Equations 14 and 15 indicate that, the active power is dependent on d-axis current while the reactive power is dependent on q-axis current. Similarly, the DC power is given by;

$$P_{dc} = V_{dc}i_{dc} \quad (16)$$

Equating equation 14 and 16 yields;

$$\frac{3}{2}Vdi_d = V_{dc}i_{dc} \quad (17)$$

Applying the kirchoff's current law at the node on the dc of fig. 1, yield the equation 18 below;

$$C \frac{du_{dc}}{dt} = i_{dc} - i_L \quad (18)$$

Where i_{dc} Converter output DC current

i_L - DC current through DC link

C_{dc} - DC capacitor capacitance

Rearranging equation 18 yields equation 19,

$$i_{dc} = C \frac{du_{dc}}{dt} + i_L \quad (19)$$

Replacing equation 17 with the values of i_{dc} in equation 19, gives equation 20.

$$\frac{3}{2}Vdi_d = V_{dc} \left\{ C \frac{du_{dc}}{dt} + i_L \right\} \quad (20)$$

Using the basic Laplace transformation and solving for U_{dc} in eqn.20, we get

$$U_{dc} = \frac{1}{c.s} \left\{ \frac{3Vdi_d}{2V_{dc}} - i_L \right\} \quad (21)$$

The resulting block diagram of the dc voltage controller loop is illustrated in Fig. 4. The disturbance introduced by i_L can be eliminated by introducing a compensation term before the converter.

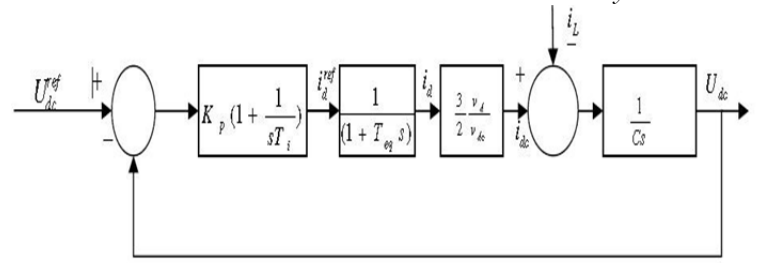


Fig. 4 DC voltage control loop in dq axes.

C. TUNING THE DC VOLTAGE CONTROLLER USING THE SYMMETRICAL OPTIMUM CRITERION

Tuning of the DC voltage control is critical in maintaining the reactive power at desired levels otherwise a slight change in DC voltage may lead to system instability. The tuning of the DC voltage controller is based on symmetrical optimum tuning where the controlled system has one dominant time constant and other minor time constant. The PI controller can be tuned using the modulus optimum criteria however, when one of the poles is already near to the origin or at the origin itself, the pole shift does not change the situation significantly. The open loop transfer function of the voltage controller already has two poles at the origin. An alternative criterion to tune the controllers in this condition is given by the symmetrical optimum criteria. As in fig. 4. Below DC voltage controller loop has a pole at the origin and thus the optimum symmetrical tuning is used in this study to design the controller's parameters. Various researches has been carried out concerning the tuning of the DC voltage controller based on optimum symmetrical tuning [14] and [15], as such, the equation below holds true.

$$Ti = a^2Teq \quad (22)$$

Ti is the proportional time constant. It is also recommended that a is between 2 and 4, thus, the equivalent time delay Teq due to the current control loop is given in equation 23 below.

$$Teq = aTa = 2Ta = 2 * \frac{1}{2fs} = 2 * \frac{1}{2*5000} = 0.0002 \quad (23)$$

Where fs is the switching frequency. If a=3 then,

$$Ti = 3^2 * 0.0002 = 0.0018 \quad (24)$$

In this study, the parameters below were utilized for the proposed VSC-HVDC controllers.

V dc = 81.7kV

V d = V = 45kV.

C = 53.933uF

Based on the symmetrical optimum tuning, the proportional gain becomes;

$$Kp = \frac{2}{3} \frac{V_{dc}C}{V_{dc}Teq} = 0.109 \quad (25)$$

$$K = \frac{3KpVd}{2*2V_{dc}} = 0.03 \quad (26)$$

$$KTiS = 0.03 * 0.0018 = 5.4 * 10^{-5} \quad (27)$$

Now, using the PI controller parameters, the overall closed loop transfer function for fig. 5, becomes,

$$Gcl = \frac{K+KTiS}{K+KTiS+TiCS^2+TiTeqCS^3} \quad (28)$$

$$Gcl = \frac{0.03+5.4*10^{-5}S}{0.03+5.4*10^{-5}S+9.7*10^{-8}S^2+1.9*10^{-11}S^3} \quad (29)$$

V. METHODOLOGY

The foregoing discussion analyzed in detail the performance of the VSC outer controllers and vector current controllers. Outer controllers perform important task of ensuring that active and reactive power flow between converters and grid is kept under control at all times. Further, they maintain the DC voltage and frequency within the standard acceptable levels. It is therefore paramount that the outer controllers are selected carefully by ensuring that they have slower response than the inner current controllers. This ideology is discussed in [11] and [16].

A. Proposed Controller

The system under study is shown in fig. 5 with two converter stations. The controller system is linked to outer and inner current controllers. The outer controllers generate the reference d-q currents components. In load flow analysis, there are six possible control mode that can be selected at any given time per converter station however, in this study two

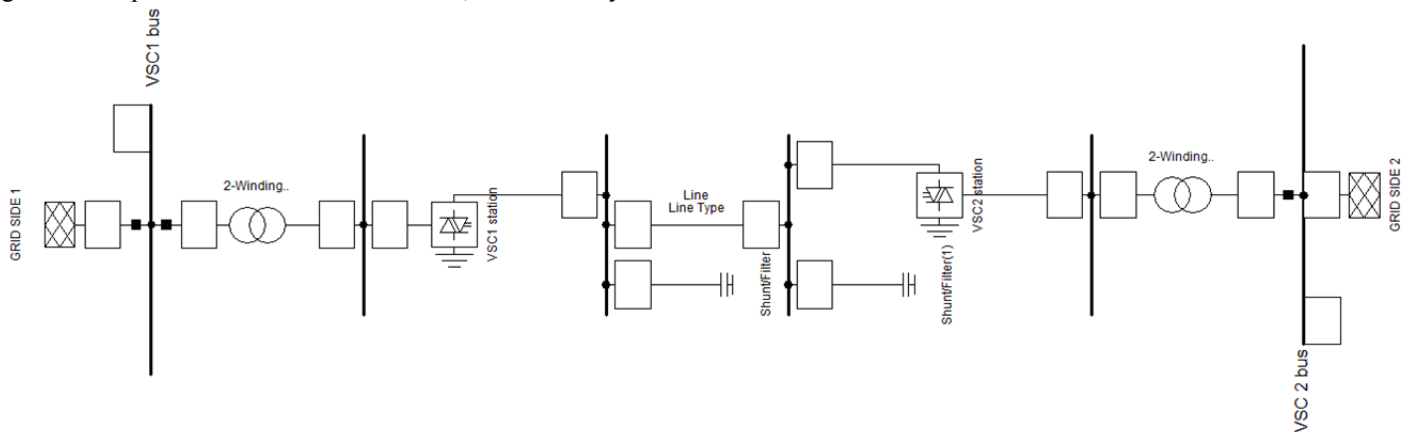


Fig. 5 VSC HVDC controller system

VSC-HVDC system has advantages over any other available mode of power transmission and therefore the designed system is expected to perform the following roles;

- i. Independent control of active and reactive power,
- ii. Capability of controlling active power in either direction,
- iii. The reactive power control at either ends must be carried out independent of each other,
- iv. Ability to control grid voltage level thus reducing losses in the connected grid.

A. Active power direction reversal

The designed VSC-HVDC controller is tested to show its effectiveness in regard to the active power variation on other parameters of interest. The active power reversal at PQ controller took place at 3 sec and 5sec respectively. The active power is reversed from -1 P.u to 1 P.u as shown in fig. 6.

control modes are selected because they cut across the other six control strategies. The two control strategies employed are:
Strategy 1: PQ control on inverter station and Vdc-Q control on rectifier station

Strategy 2: PQ control on inverter station and Vac-Vdc on rectifier station

All outer controllers are implemented by PI controllers where the difference between the reference value and the actual value is fed into the controller and the reference d-q axis currents.

B. Transient stability

The proposed VSC-HVDC system is subjected to a three phase to ground fault to analyze the controller's performance ability to respond to such disturbance and restore the system to stability.

VI. SIMULATION RESULTS

In this study two control strategies were selected per converter to analyze the grid performance both under normal conditions and under faults. The proposed VSC-HVDC controllers are implemented on DigSilent PowerFactory. Load flow was run to test the performance of the proposed VSC-HVDC controller as shown in fig.5 below.

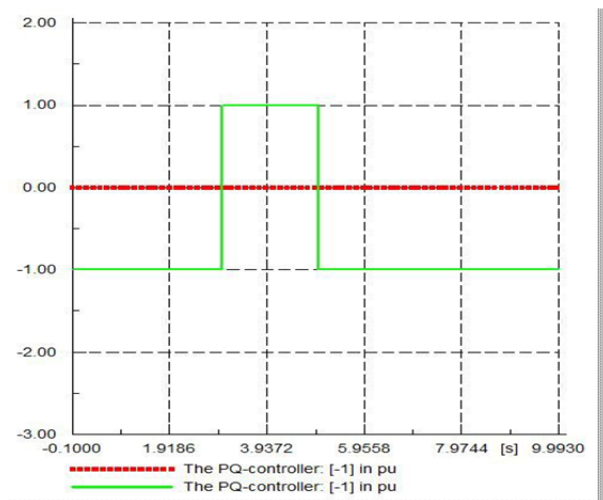


Fig. 6 PQ controller

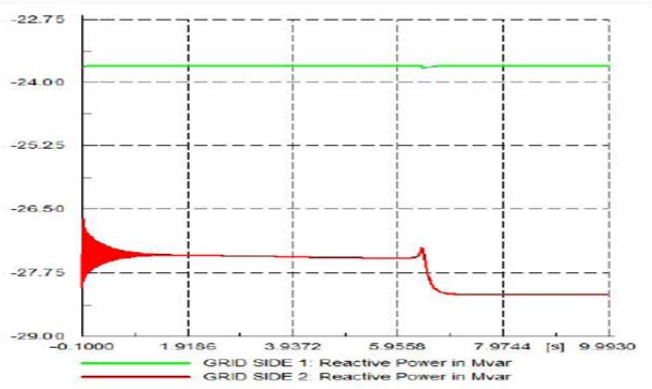


Fig.7. Reactive power in Mvar

Fig. 7 shows that the reactive power change at the two grids is slightly small except for some transients; it therefore means that the reactive power control is independent of the active power.

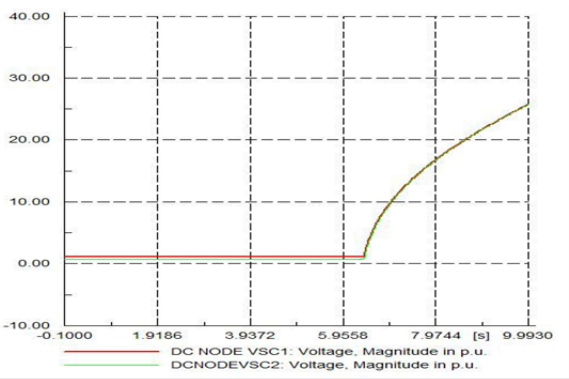


Fig. 8 DC node voltage in pu

Fig. 8 shows that the DC link bus voltages are at the desired value of 1pu and are thus not affected by the parameter event between 3 and 5 seconds respectively.

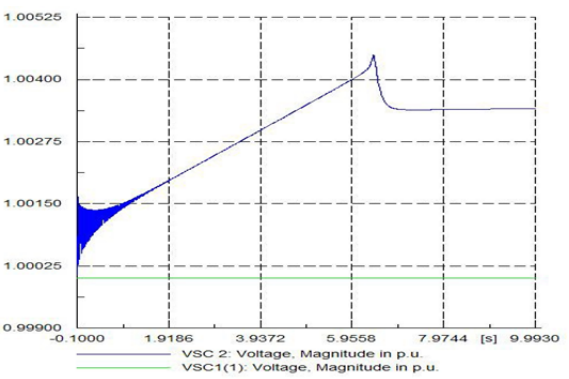


Fig. 9 VSC voltage in pu

Fig. 9 shows a slight change in voltage for VSC 2 because the occurrence of the event is near this bus while VSC 1 has no voltage variation. This behavior shows that a change in voltage has impact on reactive power changes more than the active power.

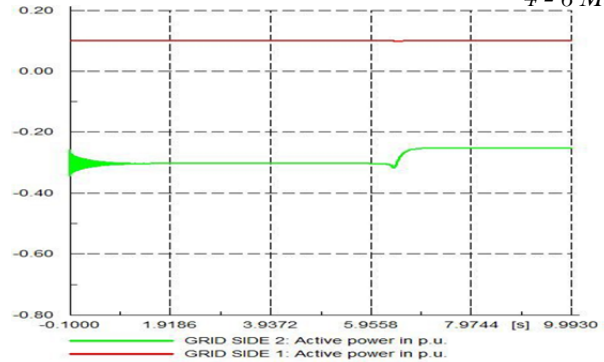


Fig. 10 Active power controller

Fig. 10 shows active power reversal as ordered by the PQ controller in fig.11. This proves that active power and reactive power are independently controlled.

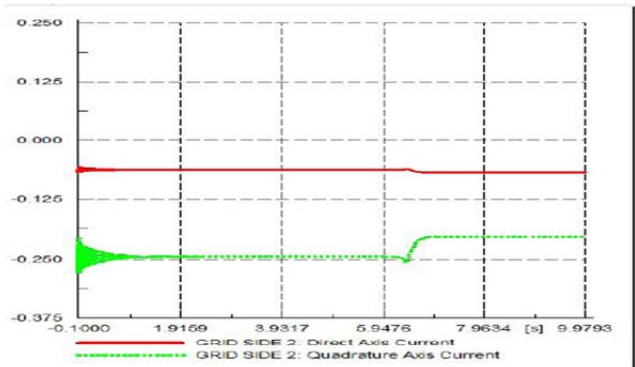


Fig. 11 Inner current controller.

Fig.11 shows an inner current controller with some variations on the q-axis current components and less variation on d-axis current components in response to the active power reversal. This is a true reflection of the independent control of reactive and active power. It also demonstrates that reactive power is dependent on q-axis components while active power depends on d axis current component. The stability of the controller was attained.

B. Reactive power flow direction reversal

Reactive power control is a continuous process carried out in a transmission system. In this study, the reactive power is delivered to the AC system by VSC through the control of phase and magnitude of the converter voltage. Therefore, the ability to control reactive power is important to any applications and the system voltage is dependent on the reactive power in the system. The reactive power reversal at PQ controller took place at 3 sec and 5sec respectively. The reactive power is reversed from 1pu to -1 pu as in fig. 12

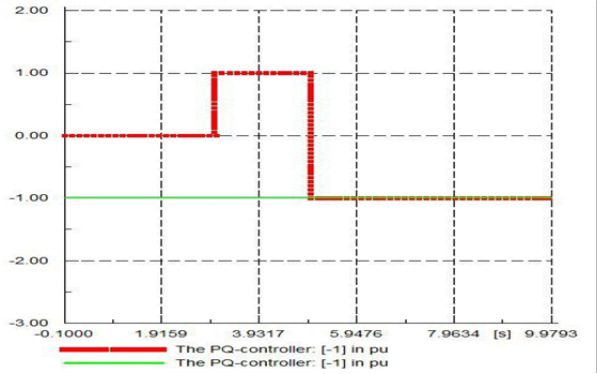


Fig. 12 PQ controller

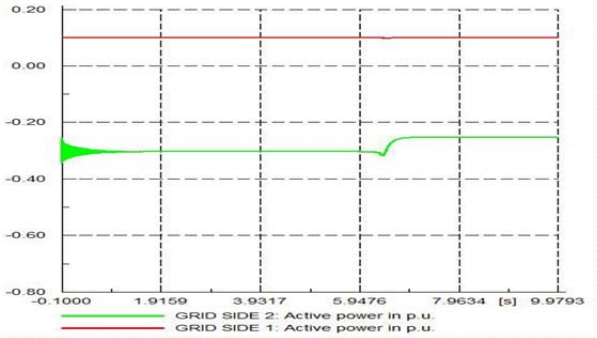


Fig. 13 Active power controller

Fig. 13 shows very slight variations in active power. This is what is expected of a well designed VSC-HVDC system whereby the active and reactive powers are independently controlled.

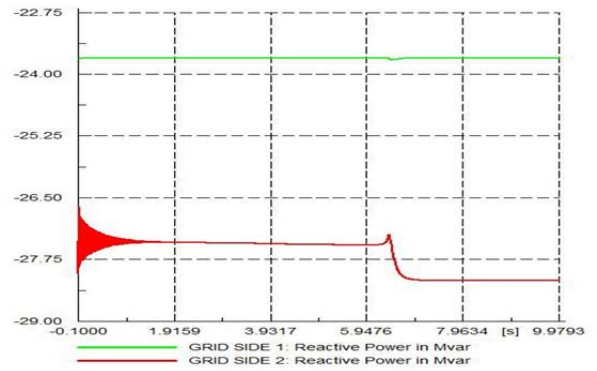


Fig. 14 Reactive power controller

Fig.14 shows reactive power changes at grid side 2 while at grid side 1, there is no variation in reactive power. This is a confirmation that the reactive power at the two grids is independent of each other.

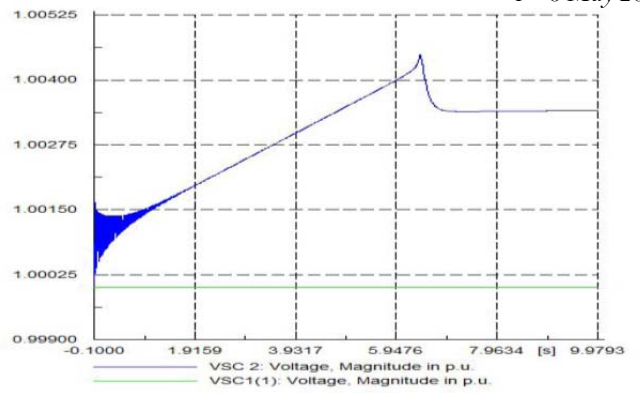


Fig. 15 VSC voltage magnitude

Fig. 15 shows that the converter bus voltage at VSC (2) shows a quick rise from its pre-disturbance value. When the reactive power returns to its pre-disturbance value, VSC(2) bus voltage returns to a value close to 1pu (nominal value). This is an indication that the dependency of bus voltage on the reactive power injected or absorbed to/from it. Consequently, the bus voltage at VSC1 (1) shows no change due to the fact that the reactive power at this side indicated no change. Hence, during contingencies Transmission system operator monitor system voltage by adjusting the reference reactive power set value until desired system voltage is achieved.

C. DC voltage step responses

In this case, at 3 s the dc reference value, $V_{dc,ref}$ is increased from 1 pu value to a value 1.5 pu and then at 5s the value is again reduced to the value 1pu. It is a normal practice for Transmission Company to transfer the powers across the Dc link at a certain DC voltage; this can be done through changing the DC voltage reference value as shown in fig. 16.

Fig.17 shows small variations which quickly track the pre disturbance value. Other simulations such as in fig. 18 and fig. 19 shows very slight variations and are thus insignificant.

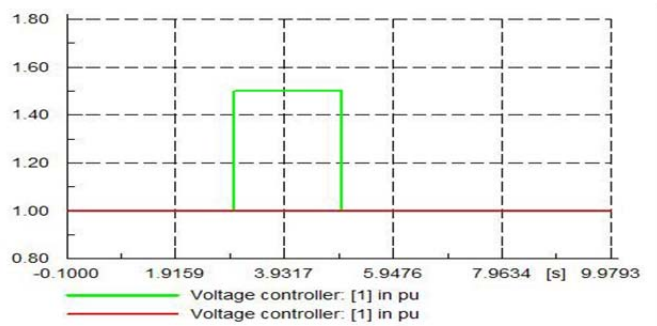


Fig. 16 Voltage controller

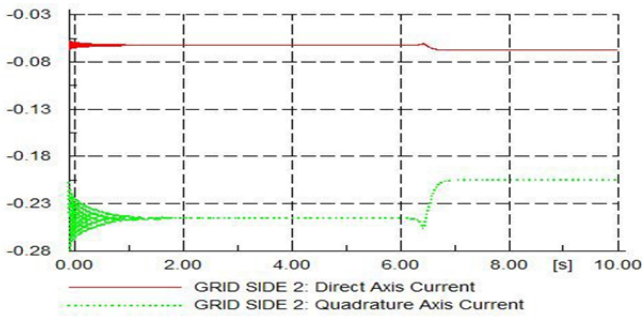


Fig.17 Inner current controller.

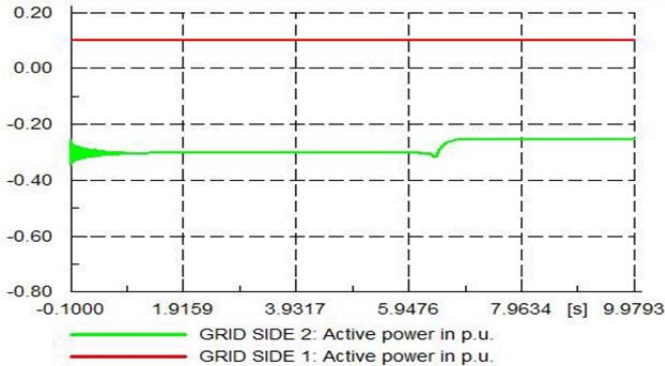


Fig. 18 Active power controller

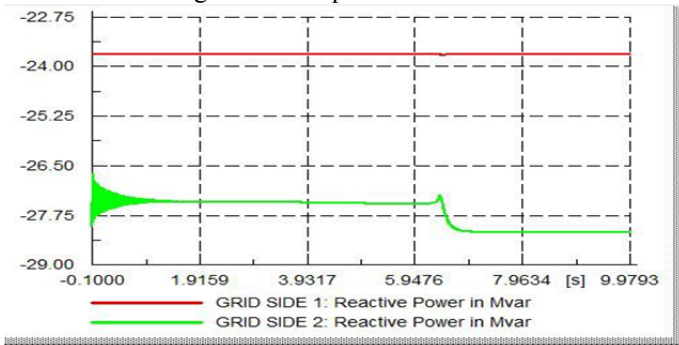


Fig. 19 Reactive power controller.

D. Transient Fault On VSC 1

In this study, the transient fault initiated on VSC 1 is a three phase to ground fault. This is a common fault in a power system. One of the major tasks of VSC-HVDC controllers is to independently control active power and reactive power. It is therefore critical to test the performance of the designed VSC-HVDC controllers during the fault and after clearance of the fault.



Fig. 20 Active power controller

Fig. 20 shows that the active power is reduced to zero on grid side 1 for the period of the fault while the active power on grid side 2 is maintained at pre disturbance value. This is an indication of the delivery of active power to the DC bus capacitors which results in no power flows to grid side-1.



Fig. 21 Reactive power controller.

Fig.21 indicates that the reactive power is maintained at zero on grid side 1 though there were some slight variations during the occurrence of the fault. The Q controller at VSC 1 ensured that the reactive power is well controlled at Zero Mvar.

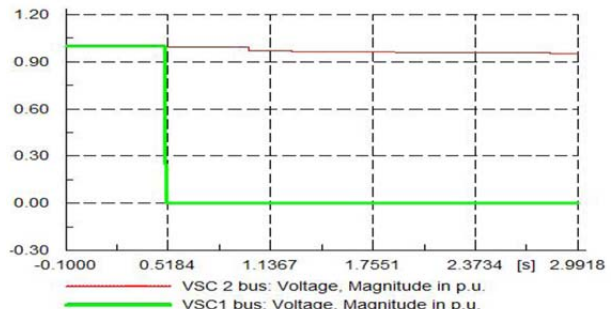


Fig. 22 Bus voltage magnitude.

Fig. 22 shows that the DC voltage on grid side 2 is maintained at 1 p.u during the fault an indication that a fault on grid side 1 has no effect on grid side 2 thus, the voltage controller designed functioned as desired.

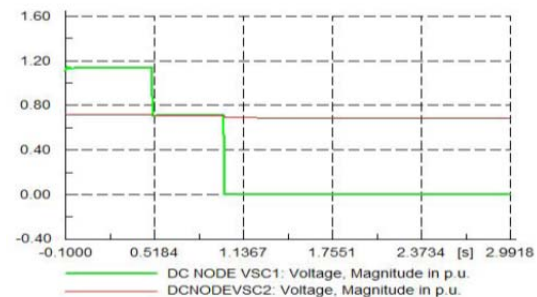


Fig. 23 Dc node voltage

Fig. 23 shows that the DC node voltage on grid side 2 was maintained at the desired value while that on grid side 1 had variation during the period of the fault and after the fault clearance the Dc node voltage was maintained at constant value.

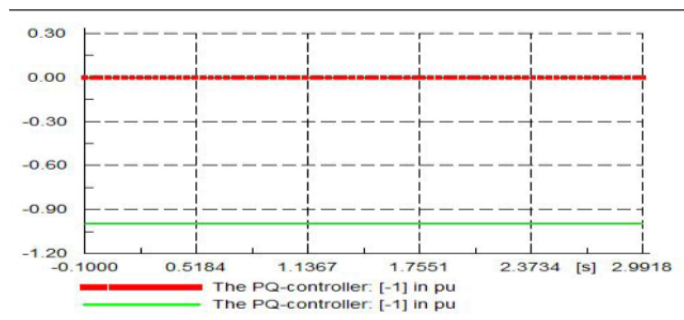


Fig. 24 PQ controller

Fig.24 shows that the PQ controller performed its function by independently controlling the active and reactive power and thus there was no variation on the PQ simulations.

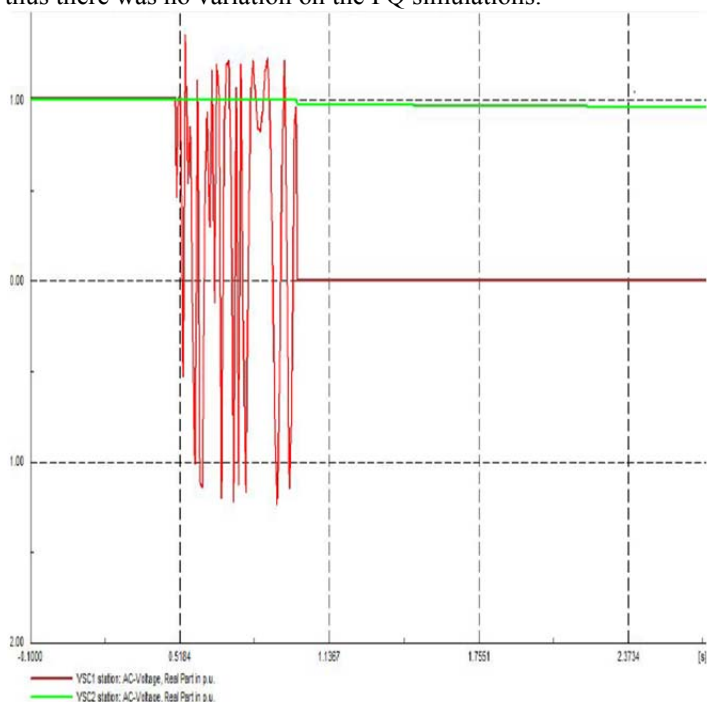


Fig. 25 AC voltage behavior under fault

Fig. 25 shows the behavior of VSC 1 and VSC 2 under a three phase fault on VSC 1. It can be seen from Fig. 25 that the VSC link is able to maintain the AC voltage undisturbed on the inverter side. The voltages and currents on VSC-2 side follow their initial operating conditions after the fault is removed.

VII. DISCUSSION

Figs. 6-24 show the performance of the proposed VSC- HVDC controllers under steady conditions aimed at reviewing the performance of the proposed VSC-HVDC transmission system. From the simulations, it is clear that the VSC-HVDC controllers have been adequately designed. This is validated by the ability of the outer and inner controllers to perform their control tasks. For example, the PQ controller designed is able to control the active and reactive power independently by ensuring that what happens on one grid has no impact on the other grid. This ensures that the power flow balance is maintained thus reducing the losses that would have been generated by the unbalanced powers. The voltage controller

maintained the DC voltage constant by controlling the reactive power flow in the power network.

Figs.21-25 shows the performance of the designed VSC-HVDC controllers under three phase fault. Transient faults are the most occurrence faults in transmission system and it is therefore important to test the designed controllers on whether they can withstand the pressure that comes with fault and be in a position to perform their task as desired during fault. A three phase short circuit fault was initiated on grid side 1 and on simulation of the event, it was realized that the active power, reactive power and DC voltages were not affected on grid side 2 however, these parameters were affected on grid side 1 for the duration of the fault and after fault clearance, normalcy was restored and system stability attained.

VIII. CONCLUSION

In this paper, it has practically been shown through simulations in DiGSilent PowerFactory that, the proposed VSC- HVDC controllers can control active and reactive power independently with ease. The designed VSC-HVDC controllers were tested under three phase short circuit fault and were found to be very effective in controlling the active and reactive power independently.

REFERENCES

- [1] M. Liserre, “innovative control techniques of power converters for industrial automation”, Journal of Electrical Engineering, 2001.
- [2] K. Mohamed, Z. Ahmed, H. Samir, F. M. Karim, and A.Rabie, “performance analysis of a voltage source converter (VSC) based HVDC transmission system under faulted conditions” Leonardo Journal of Sciences, Issue 15, ISSN 1583-0233, pp. 33–46, 2009.
- [3] W. Wang, M. Barnes, O. Marjanovic, and O. Cwikowski, “Impact of dc breaker systems on multi- terminal VSC-HVDC stability,” Impact of DC Breaker Systems on Multi- Terminal VSC-HVDC Stability, 2015.
- [4] Y. Ming, L. Gengyin, L. Guangkai, L. Haifeng, and Z. Ming, “modeling of VSC-HVDC and its active power control scheme, in power system technology,” vol. 2, pp. 1351–1355, 2004.
- [5] D. J. A. Alseid and A. Starkey, “small signal modelling and stability analysis of multiterminal VSC-HVDC, in power electronics and applications Applications (EPE 2011), Proceedings of the 11-14th European Conference on, 30 2011, pp. 1–10.
- [6] L. Xu and L. Fan, “system identification based VSC-HVDC dc voltage controller design,” IEEE, 2012.
- [7] W. X. A. Moawwad, M. S. Moursi and J. L. Kirtley IEEE Transactions on power systems, vol. 29, no.5, pp. 2478–2488, 2014.
- [8] M. B. O. M. W. Wang, A. Beddard, “Analysis of active power control for VSC-HVDC,” tech. rep., The University of Manchester, 2014.
- [9] C. Schauder and H. Mehta, “vector analysis and control of advanced static var compensators,” Proc. Inst. Elect. Eng., Gen. Transm. Distrib. vol. 140, pp. 299–306, 1993.
- [10] J. Svensson, “synchronisation methods for grid-connected voltage source converters” IEE Proc. Gener., Transm., Distrib., vol. 148,no.3, pp. 229– 235, 2001.
- [11] J. B. A.S. Elansari, S.J. Finney and M. F. Edrah, “Frequency control capability of VSC-HVDC transmission system,” AC and

- DC Power Transmission, 11th IET International Conference on, ISBN: 978-1-84919-982-7, vol. 10, pp. 1–6, Feb, 2015.
- [12] J. S. Cole and R. Belmans, “Generalized dynamic VSC MTDC model for power system stability studies,” *IEEE Transactions on power systems*, vol. 25, No.3, pp. 1655–1662, 2010.
- [13] N. K. M.R. Hassan. L. Vanfretti, L. Wei, “Generic high level VSC-HVDC grid controls and test systems for offline and real time simulation,” *Electric Power Quality and Supply Reliability Conference (PQ)*, ISBN: 978-1-4799-5020-1, pp. 57–64, 2014.
- [14] S. Preitl and R. Precup, “an extension of tuning relations after symmetrical optimum method for pi and PID controllers” *Automatica*, vol. 35, pp. 1731–1736, 1999.
- [15] P. S. O. Aydin, A. Akdag and N. Hugo, “optimum controller design for a multilevel AC-DC converter system” *Proc. Of Twentieth Annual IEEE Applied Power Electronics Conference and Exposition, APEC*, vol. 3, pp. 1660–1666, 2005.
- [16] E. A. Z. Chengyong, “parameters optimization of VSC-HVDC control system based on simplex algorithm,” in *Power Engineering Society General Meeting*